

Strong clustering of underdense regions and the environmental dependence of clustering from Gaussian initial conditions

Umami Abbas¹ and Ravi K. Sheth^{2*}

¹*Laboratoire D’Astrophysique de Marseille, Traverse du Siphon, B.P. 8, 13376 Marseille Cedex 12, France*

²*Department of Physics & Astronomy, University of Pennsylvania, 209 S. 33rd St., Philadelphia, PA 19104, USA*

13 June 2021

ABSTRACT

We discuss two slightly counter-intuitive findings about the environmental dependence of clustering in the Sloan Digital Sky Survey. First, we find that the relation between clustering strength and density is *not* monotonic: galaxies in the densest regions are more strongly clustered than are galaxies in regions of moderate overdensity; galaxies in moderate overdensities are more strongly clustered than are those in moderate underdensities; but galaxies in moderate underdensities are *less* clustered than galaxies in the least dense regions. We argue that this is natural if clustering evolved gravitationally from a Gaussian field, since the highest peaks and lowest troughs in Gaussian fields are similarly clustered. The precise non-monotonic dependence of galaxy clustering on density is very well reproduced in a mock catalog which is based on a halo-model decomposition of galaxy clustering. In the mock catalog, halos of different masses are all about 200 times denser than the critical density, and the dependence of small scale clustering on environment is entirely a consequence of the fact that the halo mass function in dense regions is top-heavy—another natural prediction of clustering from Gaussian initial conditions.

Second, the distribution of galaxy counts in our sample is rather well described by a Poisson cluster model. We show that, despite their Poisson nature, correlations with environment *are* expected in such models. More remarkably, the expected trends are very like those in standard models of halo bias, despite the fact that correlations with environment in these models arise purely from the fact that dense regions are dense because they happen to host more massive halos. This is in contrast to the usual analysis which assumes that it is the large scale environment which determines the halo mass function.

Key words: methods: analytical - galaxies: formation - galaxies: haloes - dark matter - large scale structure of the universe

1 INTRODUCTION

This is the third in a series of papers which study the environmental dependence of galaxy clustering. In hierarchical models, there is a correlation between fluctuations on different scales. This induces correlations between halo mass and/or formation and the larger scale environment of a halo (Mo & White 1996; Sheth & Tormen 2002) which, in turn, induce correlations between galaxies and their environments (Sheth, Abbas & Skibba 2004; Abbas & Sheth 2005). Abbas & Sheth (2006) showed that halo bias—the correlation between halo mass and environment—was able to account for

the environmental dependence of clustering in the Sloan Digital Sky Survey (hereafter SDSS). In that study, a galaxy’s environment was defined as the number of galaxies within $8h^{-1}\text{Mpc}$, and only a relatively small range of environments were considered: the two-point correlation function $\xi(r|\delta)$ of galaxies in the densest third of the sample was shown to be about five times larger than that of the full sample, whereas the galaxies in the least dense 30% were less strongly clustered on scales larger than about $0.1h^{-1}\text{Mpc}$.

In this paper we show that clustering strength is not a monotonic function of environment in the least dense regions: compared to the objects in the least dense 30% of the sample, the galaxies in the least dense 10% are *more* strongly clustered. Nevertheless, the statistical halo-bias based ef-

* E-mail: shethrk@physics.upenn.edu (RKS)

fect accounts very well for the observed non-monotonic relation between environment and clustering strength. Section 2 presents our measurements, shows that a halo-model (see Cooray & Sheth 2002 for a review) based mock catalog exhibits the same features as seen in the data. Section 3 discusses a simple model of the effect, and a final section summarizes our results and discusses some implications.

An Appendix discusses a somewhat surprising interpretation of the origin of halo bias. This is motivated by the fact that two of the distributions which have routinely been found to provide a good description of galaxy counts in cells are the Thermodynamic or Generalized Poisson distribution (Saslaw & Hamilton 1984; Sheth 1995), and the Negative Binomial distribution (Moran 1984). These distributions provide a good description of the counts in our catalog as well; they are both examples of Poisson cluster models (Daley & Vere-Jones 2003). We show that, despite their Poisson nature, Poisson cluster models are expected to show environmental effects. However, in such models, dense regions are dense because they happen to host massive halos. The standard analysis of halo bias assumes that the large scale environment determines the halo mass function, rather than the other way around. Nevertheless, we show that the expected halo bias in Poisson cluster models bears surprising similarity to the standard models of halo bias (Mo & White 1996; Sheth & Tormen 2002).

Throughout, we show results for a flat Λ CDM model for which $(\Omega_0, h, \sigma_8) = (0.3, 0.7, 0.9)$ at $z = 0$. Here Ω_0 is the density in units of critical density today, h is the Hubble constant today in units of $100 \text{ km s}^{-1} \text{ Mpc}^{-1}$, and σ_8 describes the rms fluctuations of the initial field, evolved to the present time using linear theory, when smoothed with a tophat filter of radius $8h^{-1} \text{ Mpc}$. The Very Large Simulation (VLS) we use to construct mock catalogs was made available to the public by the Virgo consortium. It was run with the same Λ CDM cosmology, and followed the evolution of 512^3 particles in a cubic box with sides $L = 479h^{-1} \text{ Mpc}$ (Yoshida et al. 2001). Dark matter halos were identified in this particle distribution using the Friends-of-Friends method. Each halo has a mass, a position and a velocity.

2 THE ENVIRONMENTAL DEPENDENCE OF ξ

To study the environmental dependence of clustering, we began with a parent galaxy catalog drawn from a parent catalog which was slightly larger than the SDSS DR4 database, and volume limited to $M_r < -19.5$. This catalog contains about 78,000 galaxies with accurate angular positions and redshifts; the associated comoving number density is $0.01 (h^{-1} \text{ Mpc})^{-3}$.

The environment of each galaxy in this catalog was defined as the number of such galaxies N_8 within $8h^{-1} \text{ Mpc}$. No attempt was made to correct for redshift space distortions, which, on these scales, should be relatively small (though not negligible; see discussion of Fig. 4 below). Figure 1 shows the distribution of densities which results. We have constructed four subsamples of this catalog on the basis of environment as follows. The lowest density environments we probe use the 10% of the objects with the fewest neighbours within $8h^{-1} \text{ Mpc}$. A slightly less severe

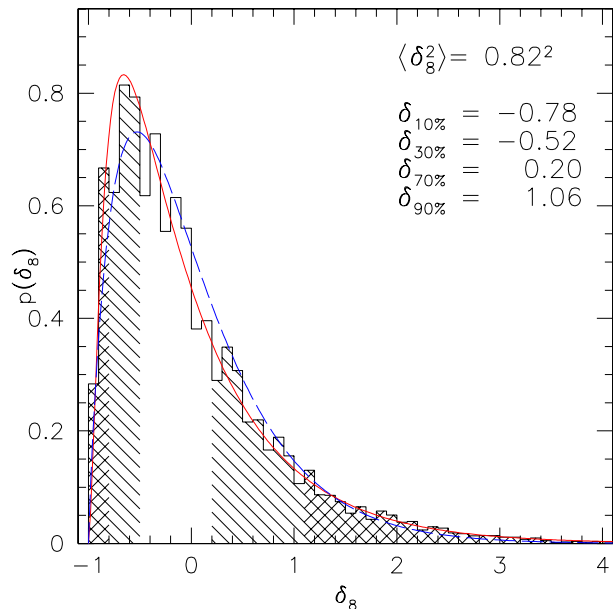


Figure 1. Distribution of galaxy overdensity in a volume limited catalog with $M_r < -19.5$ drawn from the SDSS. The density was defined by counting galaxies within $8h^{-1} \text{ Mpc}$. Dashed lines show where the area under the curve equals 10%, 30%, 70% and 90% of the total. These correspond to $\delta_8 = -0.78, -0.522, 0.196$, and 1.065 .

cut uses 30% rather than 10% of the objects. We then do the same for overdense regions: we select subsets containing 10% and 30% of the objects having the most neighbours within $8h^{-1} \text{ Mpc}$. Hashed regions indicate the various density thresholds which these cuts imply. The actual overdensity thresholds $\delta_8 \equiv N_8 / \langle N_8 \rangle - 1$ are indicated in the upper right corner of the figure, with some abuse of notation: δ_n means $n\%$ of the galaxies were in lower density environments (i.e., $p(\leq \delta_n) = n/100$). In what follows, we use these limiting values to define a number of subsamples. The Appendix discusses the solid and dashed lines; these show two Poisson cluster models that are able to provide reasonable descriptions of the measurements.

Filled circles in the right hand panel of Figure 2 show the projected correlation function of the full sample; this is computed by integrating $\xi(r_p, \pi)$ over $0 \leq \pi \leq 35h^{-1} \text{ Mpc}$. Error bars are from jack-knife resampling in which the statistics were remeasured after omitting a random region, and repeated thirty times (approximately 1.5 times the total number of bins in separation for the results presented, as in Abbas & Sheth 2006). Filled triangles show the corresponding measurement in the subsample which contains 30% of the galaxies chosen to lie in the densest regions. Filled squares show the clustering in a sample of the same size, but now drawn from the least dense regions. The open triangles and squares show the result of selecting only the densest and least dense 10%, rather than 30%, of the sample.

A number of unusual features are worth noting. First, on small scales, the correlation functions of all the subsamples have larger amplitudes than that of the parent sample from which they are drawn. This is most easily understood by supposing that the full sample is divided into two halves,

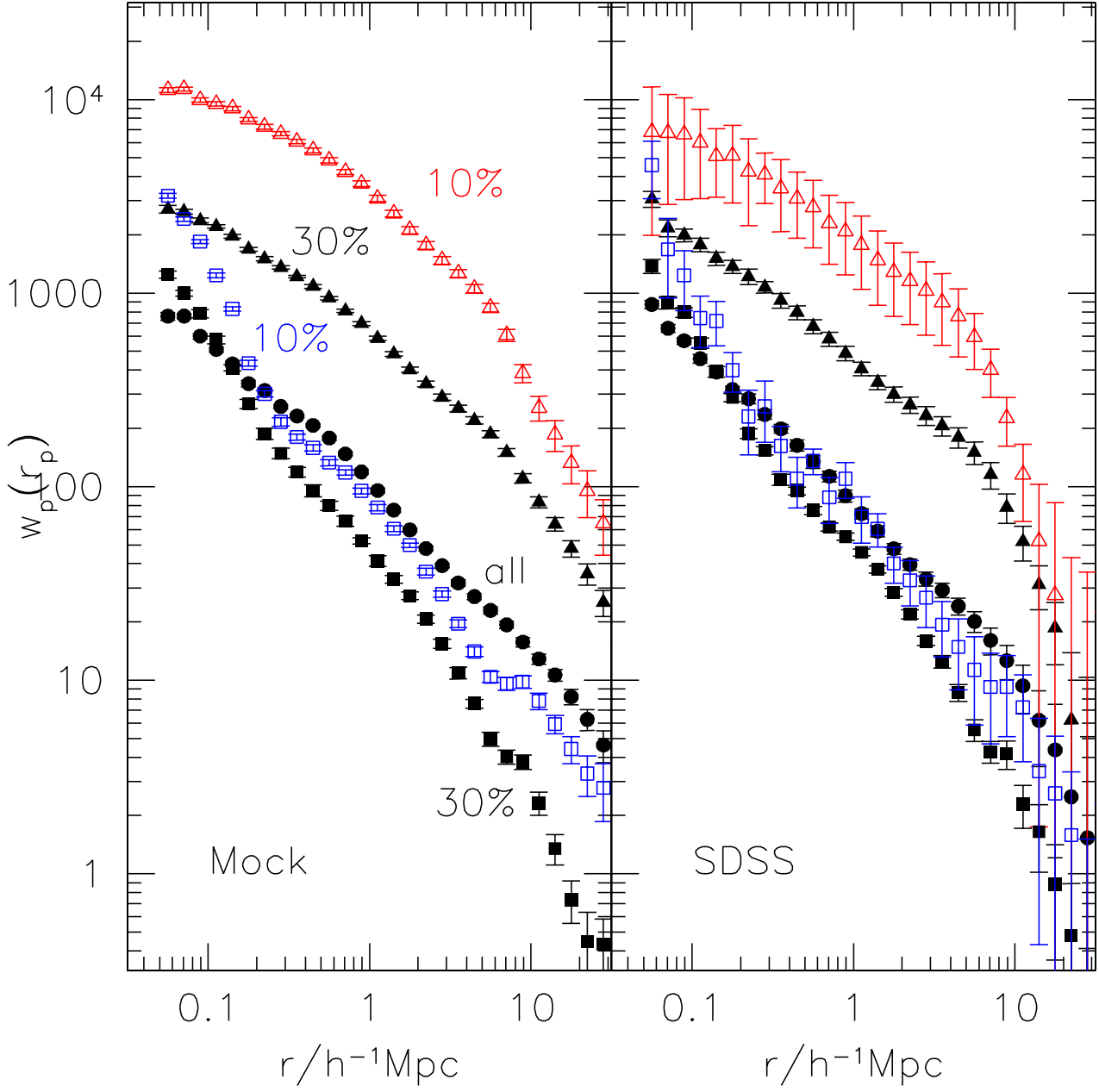


Figure 2. Environmental dependence of clustering in the SDSS for galaxies volume-limited to $M_r < -19.5$ (right) and in a halo-model based mock catalog (left). Filled circles show the clustering in the full sample; filled and open triangles show subsets containing 30% and 10% of the objects classified as being in the densest regions; filled and open squares show similar measurements but in the least dense regions.

say D and U , for dense and underdense. If the pair counts in the total sample are denoted TT , then the correlation function of the full sample is $1 + \xi_{tt} = TT/RR$, where RR denotes the counts in an unclustered distribution of the same number density. If we define ξ_{dd} and ξ_{uu} similarly, then

$$\begin{aligned} 1 + \xi_{tt} &= TT/RR = (DD + UU + 2DU)/RR \\ &= (1 + \xi_{dd})/4 + (1 + \xi_{uu})/4 + 2(1 + \xi_{du})/4. \end{aligned} \quad (1)$$

However, on scales smaller than that on which the environ-

ment was defined ($8h^{-1}\text{Mpc}$ in our case), $DU \approx 0$ by definition, so $\xi_{du} \approx -1$. In this limit, $\xi_{tt} = (\xi_{dd} + \xi_{uu})/4 - 1/2$, or

$$\xi_{dd} + \xi_{uu} = 2(1 + 2\xi_{tt}). \quad (2)$$

Thus, it is possible that ξ_{dd} and ξ_{uu} are both larger than ξ_{tt} .

Second, on small scales, ξ for the sample of galaxies in less dense regions can be substantially larger than it is for galaxies in denser regions. Abbas & Sheth (2005) argue that

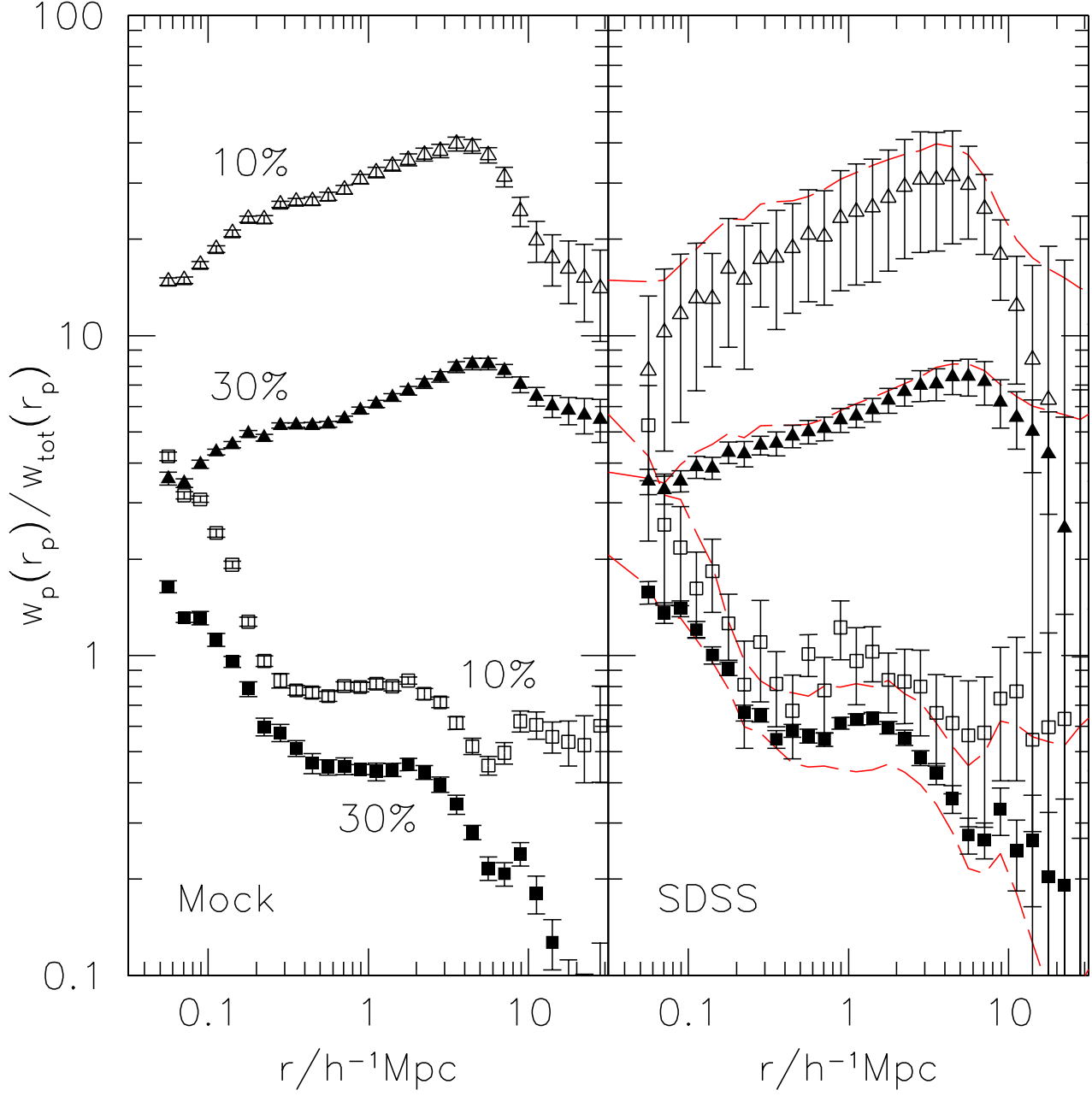


Figure 3. Same as the previous figure, but now the clustering signal is shown normalized to that for the full sample. Dashed lines in panel on the right show the loci traced out by the points shown in the panel on the left.

this would arise if the average halo mass in underdense regions is smaller than it is in dense regions (see their Section 2.2). Evidence that this is the case comes from the fact that ξ shows a feature at $\sim 0.3h^{-1}\text{Mpc}$ for the underdense sample, but not in the dense sample. Abbas & Sheth argue that this feature reflects the transition from pairs which are in the same halo to those which are in separate halos. In the underdense regions, there are few neighbouring haloes within $8h^{-1}\text{Mpc}$ (by definition), so this transition is obvious; since there may be many neighbouring halos in the dense regions, this transition is less obvious in the denser samples.

A careful inspection suggests inflection points on scales of order $2h^{-1}\text{Mpc}$ in the denser samples. If this is due to the same transition, then the radii of halos in the denser samples are about $(2/0.3)$ times larger than in the least dense sample. It is standard to assume that the halos in dense and underdense regions have the same virial densities, so our measurements suggest that the halos in dense regions are typically about $(2/0.3)^3 = 300$ times more massive than those in the least dense sample.

Finally, on larger scales where halo correlations are important, Figure 2 shows that $\xi(r|\delta)$ is strongest in the dens-

est regions. This is not unexpected in the context of the linear peaks-bias model of (Kaiser 1984), if, on average, the densest regions at the present time formed from the densest regions in the initial fluctuation field. This is because, in the initial Gaussian random field, the densest regions were more strongly clustered than regions of average density. Although the galaxies in less dense regions are less strongly clustered than those in the very dense regions, the Figure suggests that the least dense 10% are more strongly clustered than when the cut is 30%. Figure 3, which shows the ratio of $\xi(r|\delta)/\xi(r)$, shows this effect slightly more clearly. Although the difference on any given scale is only slightly larger than the error bars, it is in the same sense on all scales. (While the errors on the measured ξ are correlated between bins, the correlation between neighbouring bins is not expected to be strong, and it is expected to decrease with bin separation. In any case, the next section shows that the effect is present with much larger statistical significance in mock catalogs of the effect.)

2.1 Measurements in mock galaxy samples

A more quantitative comparison between our model and the measurements is shown in the left hand panel of Figure 2. The panel shows measurements of the environmental dependence of clustering in a mock galaxy catalog which was constructed as described by Abbas & Sheth (2006). In brief, we assigned mock ‘galaxies’ to halos in the VLS simulation by assuming that only halos more massive than a critical m_L may contain galaxies. The first galaxy in a halo is called the ‘central’ galaxy. The number of other ‘satellite’ galaxies is drawn from a Poisson distribution with mean $N_s(m)$ where

$$N_s(m) = (m/m_1)^\alpha \quad \text{if } m \geq m_L. \quad (3)$$

We distribute the satellite galaxies in a halo around the halo centre so that the radial profile follows that of the dark matter (i.e., the galaxies are assumed to follow an NFW profile). We set $m_L = 10^{11.76} h^{-1} M_\odot$, $m_1 = 10^{13.15} h^{-1} M_\odot$, and $\alpha = 1.13$; Zehavi et al. (2005) show that these choices are appropriate for this set of SDSS galaxies: $M_r < -19.5$. The resulting catalog has about 10^6 mock galaxies, because the volume of our simulation is about ten times larger than that of our SDSS catalog. This means that we can measure the environmental effects in the mock with greater precision than in the data.

The important point, which we note explicitly here, is the following: By assuming that equation (3) is the same function of m for all environments, and by assuming that the radial profile of the galaxies depends only on halo mass and not on environment, we have constructed a galaxy catalog in which all environmental effects are *entirely* a consequence of the correlation between halo mass and environment. Therefore, the loci traced out by the various sets of symbols shown in Figure 2 represent the predicted environmental dependence of ξ if there are no environmental effects other than the statistical one determined by the initial fluctuation field. The measurements in the mock catalog are extremely similar to those in the SDSS itself, leaving little room for additional environmental effects.

In the mock catalog, the halo mass function in dense regions is top-heavy. This is illustrated in Figure 4, which shows the abundance of halos per logarithmic bin in mass,

weighted by the number of galaxies in the mass bin. Symbols show this galaxy-weighted halo mass function for bins in environment, where the environment is defined by the number of neighbours N_8 in real space. Curves show the corresponding measurement when N_8 is defined (as it is in the SDSS data) from redshift space positions. Although Fingers of God tend to scatter some galaxies in massive halos into less dense environments, notice that the mix of halos is shifted towards lower masses in the less dense regions.

The precise mix of halos determines the amplitude of the correlation function on both large and small scales, so the agreement seen on all scales in Figures 2 and 3 suggests that the halo abundances shown in Figure 4 are representative of those in the SDSS: massive halos preferentially populate dense regions. Indeed, our estimate of a factor of ~ 100 difference in mass (based on Figure 2) appears to be in good agreement with the mass functions shown in Figure 4.

The fact that the mock catalog accurately reproduces the inflection in $\xi(r|\delta)$ seen at $\sim 0.3h^{-1}\text{Mpc}$ in the underdense regions has an interesting implication. Abbas & Sheth (2005) show that this inflection scale reflects the typical virial diameters of halos in these environments. Therefore, the agreement with the SDSS suggests that the mock catalog has modeled the correlation between halo mass and virial radius accurately. Since modelers differ in what this density should be (200 times background density? 200 times critical density? some other multiple of background density?), the agreement is nontrivial. In the mock, halos are 200 times the critical density whatever their mass. If they were 200 times the background density instead, they would be larger by a factor of $\Omega_0^{-1/3} \approx 3/2$. As samples get larger, $\xi(r|\delta)$ will become more precisely measured, and so it may provide an interesting constraint on halo densities.

3 LINEAR BIAS AND ENVIRONMENTAL DEPENDENCE OF CLUSTERING

The previous section showed that the large scale clustering strength is not a monotonic function of environment. A simple model of this effect follows from writing the linear peaks bias model in terms of the nonlinear density δ :

$$\xi(r|\delta) \approx \left[\frac{\delta_0(\delta)}{\sigma_\delta} \right]^2 \frac{\xi(r)}{\sigma_\delta^2} = B_\delta^2 \xi(r) \quad (4)$$

(equation 5 of Kaiser 1984 with Sheth 1998b,c), where $\delta_0(\delta)$ denotes the value of the density contrast in linear theory when the fully nonlinear overdensity is δ , and σ_δ denotes the rms value of the linear fluctuation field when smoothed on a scale which contains mass $\bar{\rho}V(1+\delta)$. For a power-law power spectrum, $\sigma_\delta^2 = \sigma_0^2/(1+\delta)^{(n+3)/3}$ so

$$B_\delta = \frac{\delta_c [1 - (1+\delta)^{-1/\delta_c}]}{\sigma_0^2 (1+\delta)^{-(n+3)/3}}. \quad (5)$$

where our relation between δ_0 and δ provides an excellent description of the spherical collapse model if we set $\delta_c \approx 1.686$. Note that, in our case, $\sigma_0 = \sigma_8 = 0.9$.

Equation (5) shows that B_δ^2 is not a monotonic function of δ , nor is it symmetric around $\delta = 0$. Figure 5 shows this explicitly for $n = -1.2$ (since this would produce a correlation function with slope -1.8 , which is approximately the slope we see for the full sample) and a few values of σ_0

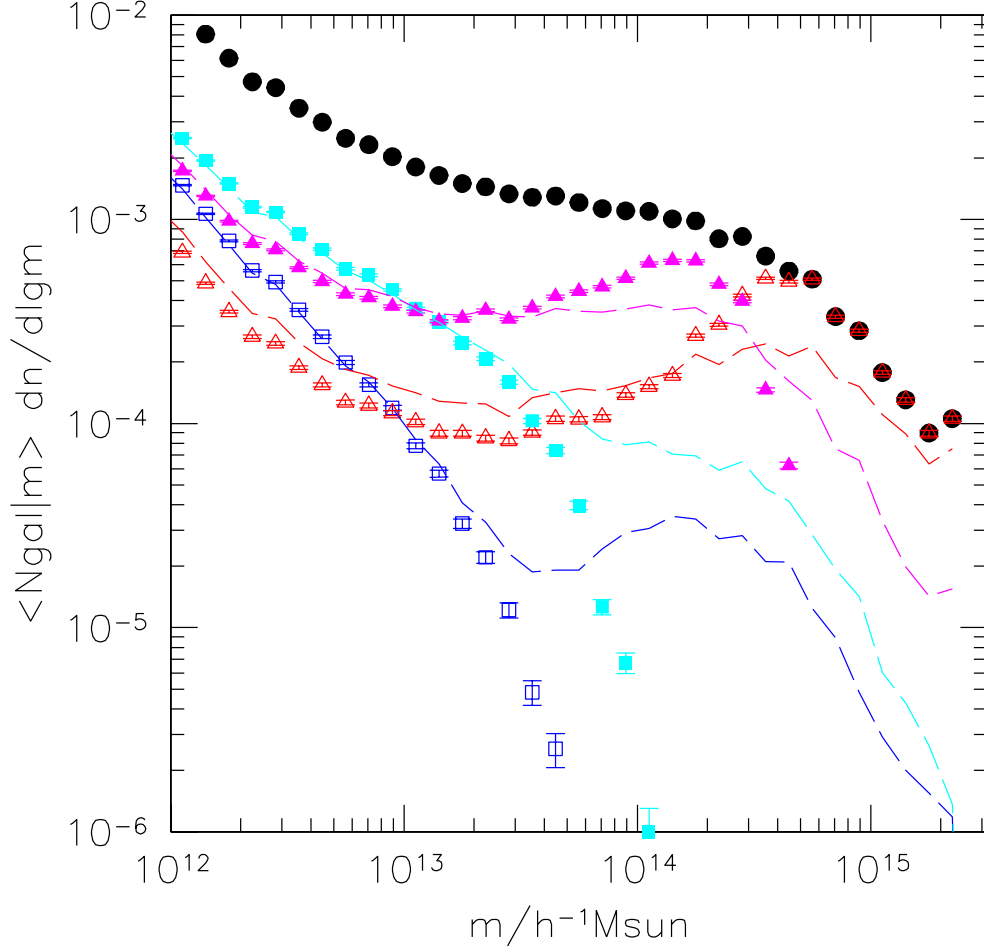


Figure 4. Galaxy-weighted halo mass function as a function of environment in our mock catalog. Filled circles show this quantity when all galaxies in the mock catalog are included. The other sets of symbols show this quantity when only galaxies in specific bins in environment are used. These bins are the 10 percent of the objects with the fewest neighbours within $8h^{-1}\text{Mpc}$ (N_8), the range between 10 and 30 percent, the range between 70 and 90 percent, and the 10 percent with the largest N_8 . Empty squares, filled squares, filled triangles and empty triangles show results for these bins when N_8 is defined using real space positions; dashed curves show the corresponding measurement when N_8 is in redshift space. In real space, objects with the lowest N_8 values populate the lowest mass halos. While this remains true in redshift space, there are a number of objects in massive halos which appear to inhabit less dense regions; these are galaxies in the Fingers of God of massive halos which reach into less dense regions.

(appropriate for a scale of about $8h^{-1}\text{Mpc}$). While this simple model is qualitatively consistent with our measurements, making a more quantitative statement is less straightforward.

The symbols show a very rough indication of the how the bias scales with environment in the previous figures. We caution that the locations of these points are *not* model free because δ in the expression above is for the dark matter, whereas our environment is defined by the galaxy distribution. To place the points on this plot, we have assumed that the galaxies in the total sample are unbiased (so $\delta = \delta_{\text{gal}}$ and ξ_{all} (the filled circles in Figure 2) equals the correlation function of the dark matter which appears in the right hand side of equation (5). For each value of δ_8 in Figure 1 we determined a δ_{gal} from requiring that $\bar{N}[1 + \delta_{\text{gal}}] =$

$(1 + \delta_8)[1 + \bar{N}(1 + \bar{\xi})]$; we used $\bar{N} = 0.014\pi 8^3/3 = 21.45$ and $\bar{N}\bar{\xi} = 1/0.2^2 - 1 = 24$, as suggested by the fact that equation (A9) with $b = 0.8$, when inserted in equation (A6), provides a good description of the distribution of N_8 in the data (c.f. solid line in Figure 1). This procedure accounts for the fact that δ_8 is computed in cells centred on galaxies, whereas δ_{gal} is not. (Equation A7 and associated discussion shows why this scaling is reasonable.) The associated bias factors for these points were read-off from the large scale values of the ratio shown in Figure 3 (recall we are assuming that the full sample is unbiased relative to the dark matter).

While the agreement is reassuring (e.g. this procedure correctly predicts *very* weak clustering for the sample which contains the 30% of the objects with lowest N_8), a better analysis of the effects of bias is required to make this model

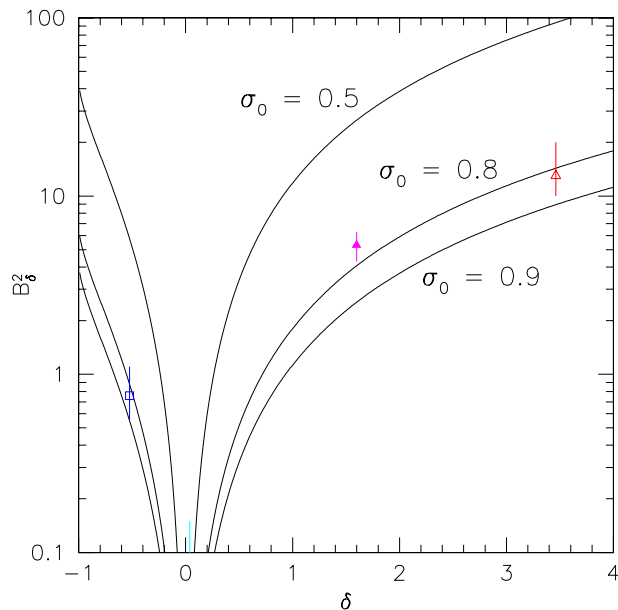


Figure 5. Bias as a function of environment. Curves show equation (5) with $n = -1.2$ and three values of σ_0 : B_δ^2 is symmetric about $\delta = 0$ for small values of σ_0 , but becomes increasingly asymmetric as σ_0 increases. Symbols (same as in Figure 3) show the bias as a function of environment derived from Figure 3 following the procedure described in the text.

more than simply illustrative. Our main point in the present work is to show that the clustering strength is not expected to be a monotonic function of environment.

4 DISCUSSION AND CONCLUSIONS

High peaks and low troughs in a Gaussian random field are similarly biased relative to the set of all fluctuations. Although nonlinear evolution destroys this symmetry, some remnants of it are expected to remain in the galaxy clustering signal (equation 5 and Figure 5). We find that galaxies in less dense regions of the SDSS are less strongly clustered than galaxies in very dense regions, but that galaxies in the least dense regions are more strongly clustered than galaxies in regions of moderate underdensity (Figures 2 and 3).

Our simple model for this effect (equation 5) makes a qualitative prediction which can soon be tested: namely, the strong clustering of underdense regions is more easily noticed when $\sigma_0 \ll 1$. This is because B_δ^2 is more symmetric about $\delta = 0$ for small values of σ_0^2 : Figure 5 shows this clearly. At fixed redshift, this means that the effect should be easier to notice for environments defined on larger scales. Alternatively, for environments defined on a fixed comoving scale, the fact that clustering is not a monotonic function of environment should be easier to notice at higher redshift. In our analysis of the SDSS, we had to go to extremely underdense environments before we found evidence that clustering was not monotonic with environment. Our model suggests that, at higher redshift, one need not go to as extreme values of δ to see the enhanced clustering of underdense regions.

We also showed that a mock galaxy catalog, constructed

to reproduce the clustering of the full sample, exhibits the same environmental dependent clustering signals as seen in the SDSS (Figures 2 and 3). This agreement is non-trivial—rather than being simple power laws with different amplitudes, the correlation functions in different environments exhibit inflections on various different scales. The agreement suggests that a number of features of the mock are also true of the Universe: namely, the mix of dark matter halo masses is top-heavy in dense regions (Figure 4), massive halos have larger virial radii, and the primary drivers of correlations between galaxy luminosity and environment are the correlations between galaxy luminosity and host halo mass, and the correlation between halo mass and environment. In particular, there is little room for the additional effects which Sheth & Tormen (2004) show may also play a role in determining these correlations (also see Gao et al. 2005; Harker et al. 2005; Wechsler et al. 2006; Zhu et al. 2006).

Environmental effects are also present in Poisson cluster models (Appendix). In such models, halo bias is simply a consequence of mass conservation: whereas the origin of halo bias is usually stated as arising from the fact that dense regions host massive halos, in Poisson cluster models, dense regions are dense precisely because they happen to host dense halos. Nevertheless, these models predict halo bias relations which are surprisingly like those in the standard model of halo bias (Mo & White 1996; Sheth & Tormen 2002). The analysis in the Appendix is particularly interesting in view of the fact that two Poisson cluster models, the Thermodynamic or Generalized Poisson (Saslaw & Hamilton; Sheth 1995) distribution and the Negative Binomial distribution, both provide good descriptions of our data (Figure 1, and also see recent analyses of the void probability function by Croton et al. 2004 and Conroy et al. 2005).

All other cosmological parameters remaining fixed, larger values of the rms fluctuation amplitude σ_8 imply a larger range of environments. So the difference between the densest and least dense regions increases with increasing σ_8 . Therefore, one might expect the environmental dependence of clustering to yield useful information about σ_8 , although the results in Tinker et al. (2006) suggest otherwise. So it is interesting that the dashed lines in Figure 3 tend to lie slightly further from unity than do the SDSS measurements. Determining whether or not this is indicating that the data prefer a value of σ_8 which is lower than the value ($\sigma_8 = 0.9$) used in the mocks is the subject of work in progress.

ACKNOWLEDGEMENTS

We thank Jeremy Tinker and Idit Zehavi for discussing the existence of this effect in their mocks, the referee P. Monaco for a helpful report, the Virgo consortium for making their simulations available to the public, Ryan Scranton for providing the SDSS data, Jeff Gardner for providing the Ntropy code which was used to measure the projected correlation functions in the simulations and the data, and the Aspen Center for Physics for hospitality while this work was completed. This work was supported in part by NSF-AST 0520647.

REFERENCES

- Abbas A., Sheth R. K., 2005, MNRAS, 364, 1327
 Abbas A., Sheth R. K., 2006, MNRAS, 372, 1749
 Conroy C., Coil A. L., White M., Newman J. A., Yan R., Cooper M., Gerke B. F., Davis M., Koo D. C., 2005, ApJ, 635, 990
 Cooray A., Sheth R. K., 2002, Phys. Rep., 372, 1
 Croton D. J., Colless M., Gaztanaga E., et al., 2004, MNRAS, 352, 828
 Daley D. J., Vere-Jones D., 2003, An Introduction to the Theory of Point Processes, Springer Series in Statistics, 2nd ed. Springer, Berlin
 Gao L., Springel V., White S. D. M., 2005, MNRAS, 363, 66
 Hamilton A. J. S., Saslaw W. C., Thuan T. X., 1985, ApJ, 297, 37
 Harker G., Cole S., Helly J., Frenk C. S., Jenkins A., 2006, MNRAS, 367, 1039
 Kaiser N., 1984, ApJL, 284, 9
 Mo H. J., White S. D. M., 1996, MNRAS, 282, 347
 Peebles P. J. E., 1980, The Large-Scale Structure of the Universe. Princeton Univ. Press, Princeton, NJ
 Saslaw W. C., Hamilton A. J. S., 1984, ApJ, 276, 13
 Sheth R. K., Abbas U., Skibba R. A., in Diaferio A., ed, Proc. IAU Coll. 195, Outskirts of galaxy clusters: intense life in the suburbs, CUP, Cambridge, p. 349
 Sheth R. K., 1995, MNRAS, 274, 213
 Sheth R. K., 1998a, MNRAS, 295, 869
 Sheth R. K., 1998b, MNRAS, 299, 207
 Sheth R. K., 1998c, MNRAS, 300, 1057
 Sheth R. K., 2003, MNRAS, 345, 1200
 Sheth R. K., Mo H. J., Saslaw W. C., 1994, ApJ, 427, 562
 Sheth R. K., Tormen G., 1999, MNRAS, 308, 119
 Sheth R. K., Tormen G., 2002, MNRAS, 329, 61
 Sheth R. K., Tormen G., 2004, MNRAS, 350, 1385
 Wechsler R. H., Zentner A. R., Bullock J. S., Kravtsov A. V., Allgood B., 2006, ApJ, 652, 71
 Tinker J., Weinberg D. H., Warren M. S., 2006, ApJ, 647, 737
 Yoshida N., Sheth R. K., Diaferio A., 2001, MNRAS, 328, 669
 Zehavi I. et al., 2005, ApJ, 630, 1
 Zhu B., Zheng Z., Lin W. P., Jing Y. P., Kang X., Gao L., 2006, ApJL, 639, L5

APPENDIX A: ENVIRONMENTAL EFFECTS IN POISSON CLUSTER MODELS

The main text argued that the correlation function depends on environment primarily because the halo distribution is top-heavy in dense regions. While it is tempting to conclude that this derives from the fact that more massive halos are more strongly clustered, this is not the whole story. The following calculation illustrates that, even in Poisson cluster models, the distribution of halos depends on environment. This is a simple consequence of mass conservation: a region containing N particles may not host a halo with mass $n > N$.

As the name suggests, Poisson cluster models are point distributions in which cluster centers are distributed at random (i.e., the distribution of clusters is Poisson); different models are distinguished by specifying the probability that a randomly selected cluster contains n galaxies. The clusters themselves are assumed to have zero size. Poisson cluster distributions are also sometimes called Compound Poisson (Daley & Vere-Jones 2003).

A1 Counts-in-cells for unclustered clusters

Let $p(N|V)$ denote the probability that a randomly placed cell (i.e. not necessarily centred on a particle) of volume V contains N particles, and define

$$P(s|V) \equiv \sum_N s^N p(N|V). \quad (\text{A1})$$

For a Compound Poisson distribution,

$$\ln P(s|V) = \bar{N} [H(s) - 1] \left[\partial H(s) / \partial s|_{s=1} \right]^{-1}, \quad (\text{A2})$$

where \bar{N} is the mean of $p(N|V)$,

$$H(s) \equiv \sum_n s^n h(n), \quad (\text{A3})$$

and $h(n)$ denotes the probability that a randomly chosen cluster contains n particles (e.g. Daley & Vere Jones 2003).

In the main text we defined the environment of a particle (in that case a galaxy) by counting the number of particles in a cell of volume V centred on it. Hence, we seek an expression for the probability $q(N|V)$ that a cell of volume V , centred on a randomly chosen particle, also contains $N - 1$ other particles. For Compound Poisson distributions, this distribution is simply related to $p(N|V)$, the distribution of counts in randomly placed cells. This is because

$$q(N|V) \equiv \frac{\sum_{n=1}^N n h(n) p(N - n|V)}{\sum_{n>0} n h(n)}; \quad (\text{A4})$$

the terms involving $h(n)$ denote the probability that V is centred on a particle in an n halo, and the term involving p denotes the probability that V contains $N - n$ particles in addition to the n which are associated with the halo in which the chosen particle sits. Note that the term in the denominator above is $\partial H(s) / \partial s$ evaluated at $s = 1$. In what follows, we will denote this quantity $H'(s = 1)$.

To derive an expression for q , it is convenient to begin with

$$\begin{aligned} Q(s|V) &\equiv \sum_{N>0} s^N q(N|V) \\ &= \sum_{N>0} s^N \sum_{n=1}^N \frac{n h(n) p(N - n|V)}{H'(s = 1)} \\ &= \sum_{N>0} \sum_{n=1}^N \frac{s^n n h(n) s^{N-n} p(N - n|V)}{H'(s = 1)} \\ &= \sum_{n>0} \frac{s^n n h(n)}{H'(s = 1)} \sum_{N>n-1} s^{N-n} p(N - n|V) \\ &= \sum_{n>0} \frac{s^n n h(n)}{H'(s = 1)} P(s|V) = s \frac{H'(s)}{H'(s = 1)} P(s|V) \\ &= \frac{s}{\bar{N}} \frac{\partial P(s|V)}{\partial s} = \frac{s}{\bar{N}} \frac{\partial}{\partial s} \sum_N s^N p(N|V) \\ &= \frac{s}{\bar{N}} \sum_{N>0} N s^{N-1} p(N|V). \end{aligned} \quad (\text{A5})$$

Comparison of the first and last expressions shows that

$$q(N|V) = \frac{N}{\bar{N}} p(N|V). \quad (\text{A6})$$

Evidently, if one only considers volumes which are centred on particles, then the distribution of counts in such cells

is simply related to the distribution of counts in randomly placed volumes—the two distributions differ by one factor of N/\bar{N} .

This useful result follows from two assumptions: clusters have vanishingly small sizes, and they are uncorrelated with one-another. So long as we restrict attention to volumes V which are large compared to the virial radius of a typical cluster (about 2 Mpc), the assumption that halos have negligible sizes should be reasonable. The neglect of cluster clustering in our Universe is less reasonable, but, as we show below, is still a useful approximation.

Equation (A5) implies that \bar{N}_q , the mean of q is

$$\bar{N}_q \equiv \frac{\langle N \rangle}{\bar{N}} + \frac{\langle N(N-1) \rangle}{\bar{N}^2} = 1 + \bar{N}(1 + \bar{\xi}) \quad (\text{A7})$$

where $\bar{\xi}$ is the volume average of the two point correlation function. This makes intuitive sense: the mean count when centred on a particle is one plus \bar{N} , plus a contribution from the fact that the particles are correlated.

A2 The Generalized Poisson and Negative Binomial distributions

In what follows, we use the cluster mass function associated with an initially Poisson distribution:

$$h(n) = \frac{(nb)^{n-1} \exp(-nb)}{n!}, \quad \text{where } b = (1 + \delta_c)^{-1} \quad (\text{A8})$$

(Epstein 1983; Sheth 1995). Here δ_c is the critical density in the initial density fluctuation field that is required for collapse in the spherical model. Thus, $b = 0$ initially, and it grows to $b \rightarrow 1$. If these clusters have a Poisson distribution, then

$$p(N|V) = \frac{\bar{N}(1-b)}{N!} [\bar{N}(1-b) + Nb]^{N-1} \times \exp[-\bar{N}(1-b) - Nb] \quad (\text{A9})$$

is the Generalized Poisson distribution (e.g. Sheth 1998b). Here \bar{N} is the average number of particles in a cell of size V : $\langle N \rangle = \bar{N}$. This distribution, which is sometimes called the Thermodynamic distribution in the astrophysical literature (Saslaw & Hamilton 1984; Sheth 1995), provides a reasonably good description of the counts of galaxies in randomly placed cells of size V (Hamilton, Saslaw & Thuan 1985; Sheth, Mo & Saslaw 1994; Conroy et al. 2006).

For this distribution, the variance is $\langle N^2 \rangle - \langle N \rangle^2 = \bar{N}/(1-b)^2$ so the mean value of q is $\bar{N} + 1/(1-b)^2$. The solid line in Figure 1 shows $q(N|V)$ associated with equation (A9), where $\bar{N} = 0.014\pi 8^3/3 = 21.45$ and $b = 0.8$. It provides a good description of the measured distribution.

The dashed line shows a similar analysis of the Negative Binomial distribution. This distribution has

$$p(N|V) = \frac{(\gamma + N - 1)!}{N! (\gamma - 1)!} \beta^\gamma (1 - \beta)^\gamma \quad (\text{A10})$$

with $\gamma \equiv \bar{N}(1 - \beta)/\beta$. The Negative Binomial is a Compound Poisson distribution with

$$h(n) = \frac{\beta^n / n}{-\ln(1 - \beta)}. \quad (\text{A11})$$

The mean and variance of this distribution are \bar{N} and $\bar{N}/(1 - \beta)$, so we have set $\bar{N} = 21.45$ as before, and $\beta = 1 - (1 - b)^2 =$

0.96 (so the variance also matches that of the Generalized Poisson distribution and the data).

Figure 1 suggests that the Generalized Poisson distribution provides a slightly better description of this dataset than does the Negative Binomial. We are not as interested in which provides a better fit, as we are in the fact that a Compound Poisson model appears to work so well.

A3 Halo bias in Compound Poisson distributions

Having made the connection between counts-in-cells and the cluster distribution, we now consider environmental effects in Poisson cluster models. The mean density of n -halos which are surrounded by regions which contain N particles on the scale V is

$$h(n|N) = \frac{\bar{n}h(n)}{\sum n h(n)} \frac{p(N - n|V)}{p(N|V)}. \quad (\text{A12})$$

The ratio of this to the average density of n -halos is $p(N - n|V)/p(N|V)$. Since this ratio is obviously different from unity, the mass function of halos in dense regions is different from underdense regions. Typically, $p(N|V)$ drops exponentially when $N \gg \bar{N}$: $p(N|V) \propto \exp(-\alpha N)$ with $\alpha > 0$. Thus, $p(N - n)/p(N) \approx \exp(\alpha n)$: massive halos are exponentially more abundant in regions with large N .

The following explicit calculation shows that the Poisson cluster model actually captures much of the usual parametrization of the environmental dependence of halo abundances. That is, the following demonstrates that mass conservation itself provides a significant source of halo bias. Since mass conservation is most important on scales V where the typical mass in a cell is not substantially larger than the typical halo mass, we expect the Poisson cluster model to provide a reasonable approximation on such scales. (And recall that Figure 1 shows that the Generalized Poisson and Negative Binomial distributions do indeed provide good descriptions of the data.)

A4 Halo bias in the Generalized Poisson distribution

If we define $NB \equiv \bar{N}(1 - b) + Nb$ (the reason for this notation will become clear shortly), then the density of n halos surrounded by regions of size V which contain N particles is

$$h(n|N) = \left(\frac{B - b}{BV} \right) \binom{N}{n} \left(\frac{nb}{NB} \right)^{n-1} \left(1 - \frac{nb}{NB} \right)^{N-n-1} \quad (\text{A13})$$

where we have used the fact that $1 - b/B = (NB - Nb)/NB = \bar{N}(1 - b)/[\bar{N}(1 - b) + Nb]$. This form is precisely that of the conditional mass function of n halos in the Poisson model (Sheth 1995, 2003). This is remarkable for the following reason.

The usual estimate of the environmental dependence of halo abundances uses the conditional mass function, and it uses the spherical evolution model to transform the density N/\bar{N} to an initial overdensity (Mo & White 1996; Sheth & Tormen 2002). To see what the transformation is in the present case, set $B = (1 + \delta_0)^{-1}$ (this is motivated by the fact that $b = (1 + \delta_c)^{-1}$). Then $B = \bar{N}(1 - b)/N + b$, so $1 + \delta_0 = (1 + \delta_c)(1 + \delta)/[\delta_c + 1 + \delta]$. Hence, in a model

in which the halos in the unconditional mass function are assumed to have a Poisson spatial distribution, the mapping between linear and nonlinear density is

$$\delta_0 = \frac{\delta_c}{1 + \delta_c/(1 + \delta)} \frac{\delta}{1 + \delta} \approx \delta_c \frac{\delta}{1 + \delta}. \quad (\text{A14})$$

This relation is qualitatively like that of the spherical model, which is very well approximated by

$$1 + \delta \approx (1 - \delta_0/\delta_c)^{-\delta_c}. \quad (\text{A15})$$

See Sheth (1998b,c) for more discussion of the similarities between this and the spherical model, and another derivation of the relation between equations (A8) and (A9). This qualitative similarity, and the fact that the Generalized Poisson model appears to describe the data in Figure 1 reasonably well, both suggest that Poisson cluster models may provide useful insight into the origin of environmental effects.

In these models, environmental effects arise not because dense regions host the most massive halos, but because a region which contains a massive halo tends to be denser than average, simply because of mass conservation. This is a rather different view of environmental effects than that of Mo & White (1996) and Sheth & Tormen (2002), where the large scale environment, rather than mass conservation, is seen as the primary driver of the correlation between halo mass and environment!

The formation histories of halos in Poisson cluster models have been studied in Sheth (1998a). By combining that analysis with the present one, it should be interesting and straightforward to see what correlations between formation history and environment are built into such models. In addition, it would also be interesting to repeat this analysis for the Negative Binomial distribution.